

Electronic Supplementary Information

Everlasting chromic acid oxidation: solar-driven recycling of hexavalent chromium ions for quinone productions

Tomohiko Nakajima,^{*a} Megumi Kanaori,^a Aya Hagino,^a Hiroyuki Tateno,^b Tetsuo Tsuchiya^a and Kazuhiro Sayama^b

^a Advanced Coating Technology Research Center, National Institute of Advanced Industrial Science and Technology, Tsukuba Central 5, 1-1-1 Higashi, Tsukuba, Ibaraki 305-8565, Japan.

^b Research Center for Photovoltaics, National Institute of Advanced Industrial Science and Technology, Tsukuba Central 5, 1-1-1 Higashi, Tsukuba, Ibaraki 305-8565, Japan.

Market for Cr(VI) compounds

The hexavalent chromium oxides are almost industrially manufactured and the trade volume has been still very large. For example, the trade volumes (value) of CrO₃ and Na₂Cr₂O₇ in the U.S. 2014 were 15.5 kiloton (67,200 thousand dollars) and 13.5 kiloton (24,400 thousand dollars).¹

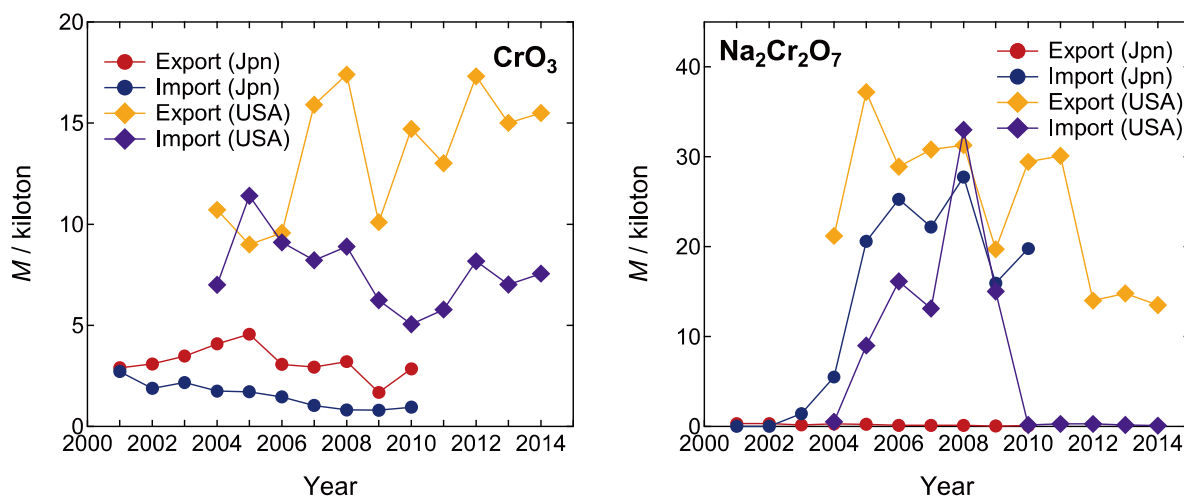


Fig. S1: The trade volume of representative hexavalent chromium oxides in Japan and United States of America.^{1,2}

Safety and health topics of Cr(VI)

The safety issues of Cr(VI) for workers have been reported by many institutes such as “Occupational Safety and Health Administration” in United States Department of Labor.

See in the webpage: <https://www.osha.gov/SLTC/hexavalentchromium/>

Phase purity, crystal structure and PEC performance of the WO₃ nanosponge photoanode

The XRD pattern of original WO₃ nanoparticles was evaluated to be a pure γ -phase of WO₃ with a monoclinic $P2_1/c$ space group. The diffraction peaks were fitted without any specific crystal orientation by Rietveld method by using RIETAN-FP program,³ and the unit cell parameters were refined to be $a = 7.3204(5)$ Å, $b = 7.5301(5)$ Å, $c = 7.6917(5)$ Å and $\beta = 90.67(1)^\circ$, which were almost consistent with the reported values (JCPDS 20-1324⁴). The WO₃ nanosponge photoanode was crystallized at 550 °C in the pure γ -phase of WO₃. The WO₃ nanosponge photoanode showed preferential (001)-orientation growth.

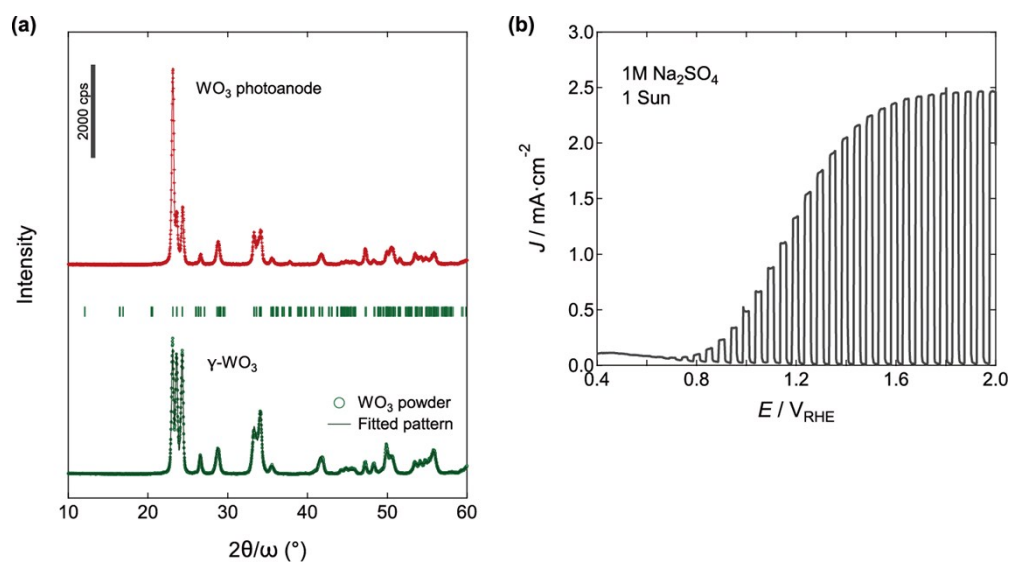


Fig. S2: (a) XRD patterns of the WO₃ nanosponge photoanode and original WO₃ nanoparticles. The diffraction pattern for the WO₃ nanoparticles was fitted by Rietveld method. The vertical marks represent the positions calculated for Bragg reflections for γ -WO₃. (b) J - V curves under chopped simulated sunlight at 1 Sun in 1 M Na₂SO₄ electrolytes from the backside of the WO₃ photoanode.

PEC measurement setup

The simulated sunlight at 1 Sun was illuminated from the backside of WO₃ nanosponge photoanode to avoid the excess absorption of illuminated light by the colored electrolytes contained Cr ions.

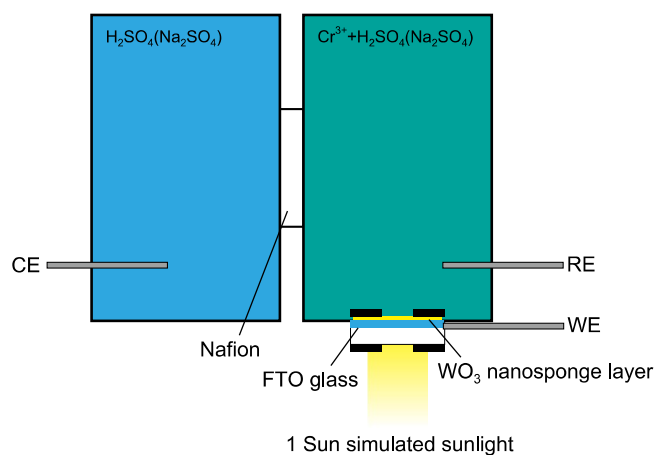


Fig. S3: The experimental setup for PEC measurements.

Spectrum of illuminated solar simulator

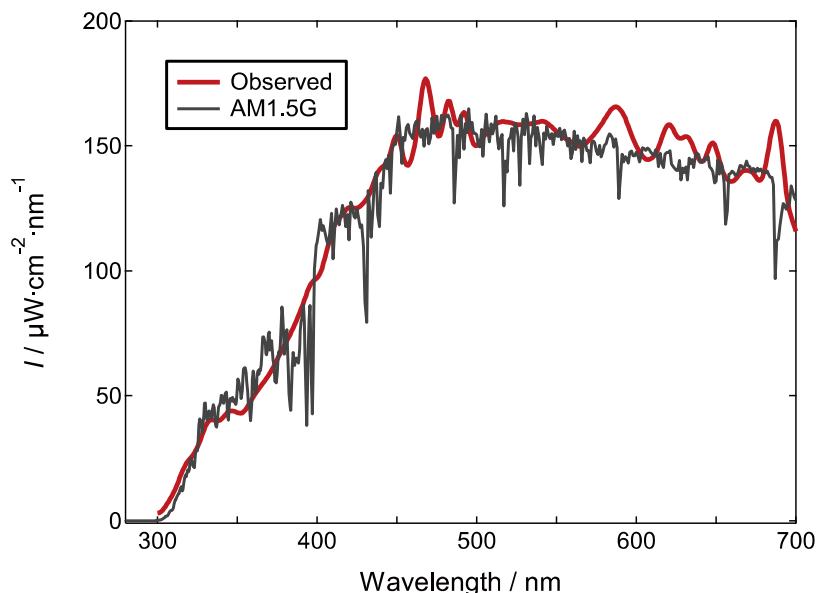


Fig. S4: The spectra for $100 \text{ mW}\cdot\text{cm}^{-2}$ AM1.5G (1 SUN) and simulated solar light from a 150 W Xe lamp (XES-40S2-CE, San-Ei Electric)

Determination of Cr^{6+} quantity in the solutions

The production of Cr^{6+} ions was evaluated by colorimetry by using the UV-VIS spectroscopy. Firstly, the absorption spectra of reference solutions for Cr^{3+} and Cr^{6+} in the aqueous sulfuric acid were measured (Figs S5a and S5b), and we confirmed that the spectral shape was almost unchanged in each sulfuric acid concentration and the intensity was just varied by the chromium ion concentrations. The reference spectra were deconvoluted, and those spectral shapes were expressed as $f_{\text{III}}(\lambda)$ for Cr^{3+} and $f_{\text{VI}}(\lambda)$ for Cr^{6+} . For the concentration analysis of Cr^{6+} in the PEC solutions, the absorption spectra of test solutions were fitted by following equation:

$$f(\lambda) = (c_{\text{III}} - c_{\text{VI}})f_{\text{III}}(\lambda) + c_{\text{VI}}f_{\text{VI}}(\lambda) - a f_{\text{III}}(\lambda)$$

where the c_{III} and c_{VI} represent the concentrations of Cr^{3+} and Cr^{6+} , and a indicates the absorption constant for initial solution of Cr^{3+} . Figure S5c shows one example of fitted test solution by using this equation. The spectral curve was fitted very well and the c_{VI} was evaluated with satisfactory accuracy.

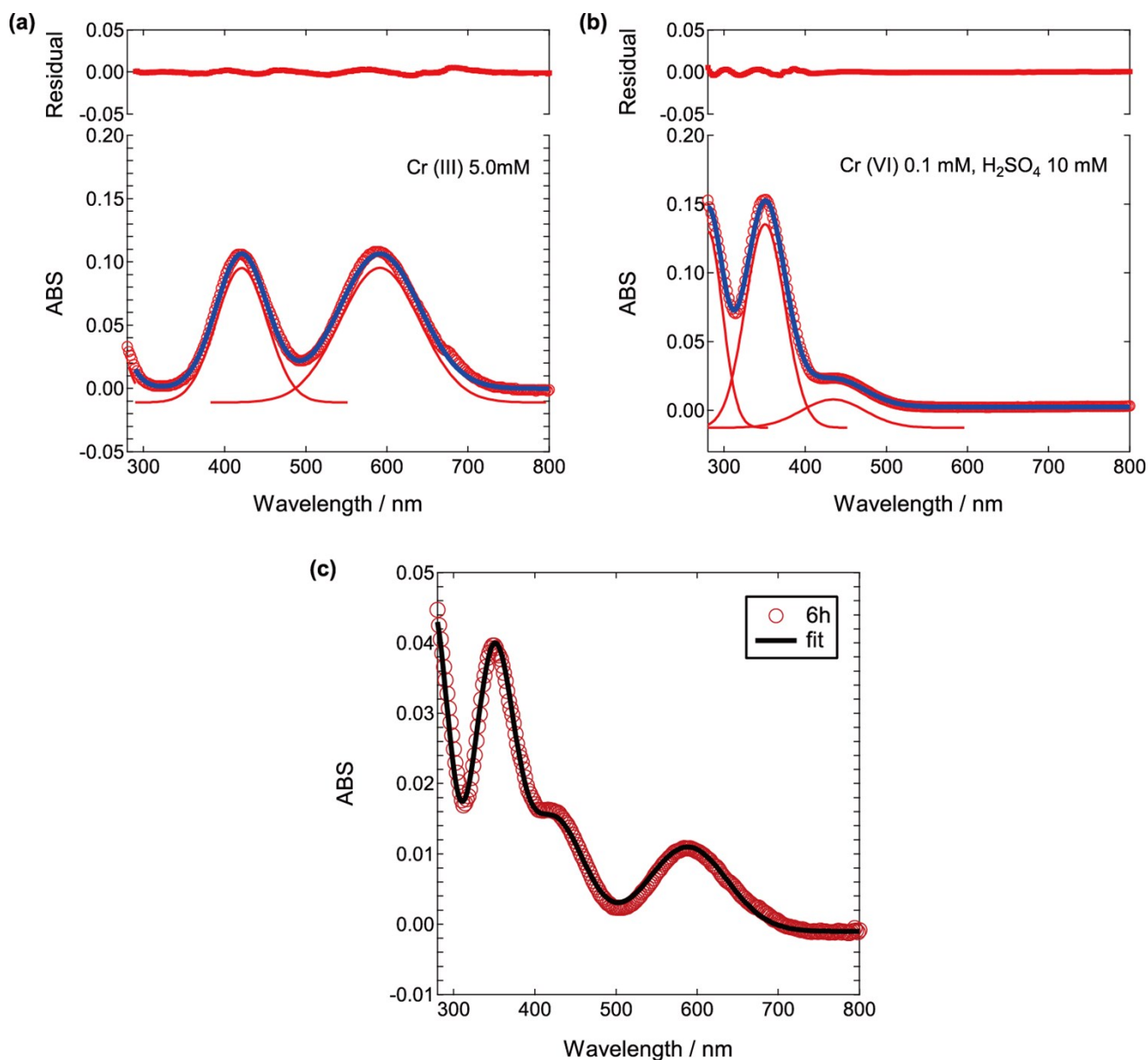


Fig. S5: The absorption spectra for the reference solutions of (a) Cr³⁺ and (b) Cr⁶⁺. (c) The fitted spectral curve of test solution after the PEC reaction.

Determination of S₂O₈²⁻ quantity in the solutions

The production of S₂O₈²⁻ was evaluated by colorimetry by using the UV-VIS spectroscopy. The obtained solution specimen was mixed with equivalent amount of 0.01M FeSO₄ and 1M H₂SO₄ solution. The optical absorbance spectra were measured after the stirring of mixed solutions, and the S₂O₈²⁻ quantity was evaluated from the absorption at 310 nm.

FESEM image for the WO_3 nanosponge photoanode

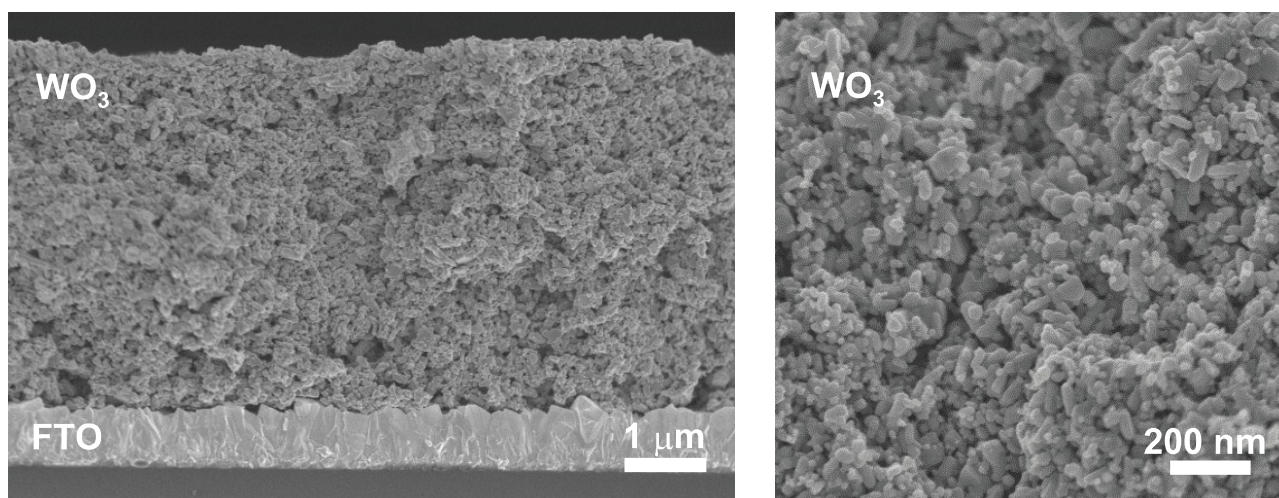


Fig. S6: Cross-sectional views of FESEM images for the WO_3 nanosponge photoanode.

$\text{S}_2\text{O}_8^{2-}$ effect on the oxidation of Cr^{3+} ions

To study the $\text{S}_2\text{O}_8^{2-}$ effect on the Cr^{3+} ions in the aqueous sulfuric acid solutions, 1 mM $\text{K}_2\text{S}_2\text{O}_8$ was added to the 10 mM Cr^{3+} and 10 mM H_2SO_4 solution. The spectral shape was not varied by the addition at all (Fig. S6), indicating no Cr^{6+} evolution. Therefore, the Cr^{6+} ions confirmed after the photoillumination to the WO_3 photoanodes was derived not from the chemical reaction (oxidation) by the simultaneously generated $\text{S}_2\text{O}_8^{2-}$ ions but from the direct photoelectrochemical reaction at the photoanode surface.

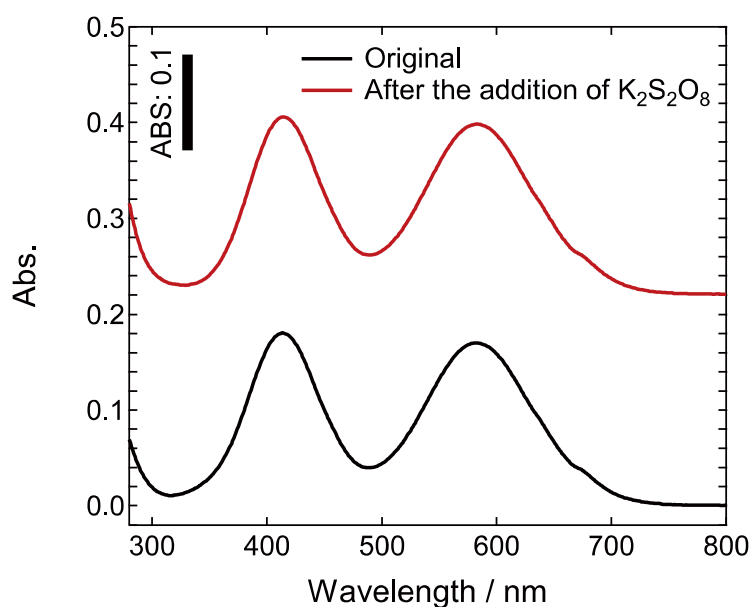


Fig. S7: The absorption spectra of 10 mM Cr^{3+} and 10 mM H_2SO_4 solutions before and after the addition of 1 mM $\text{K}_2\text{S}_2\text{O}_8$.

Cr³⁺ concentration effect on the J-V curves

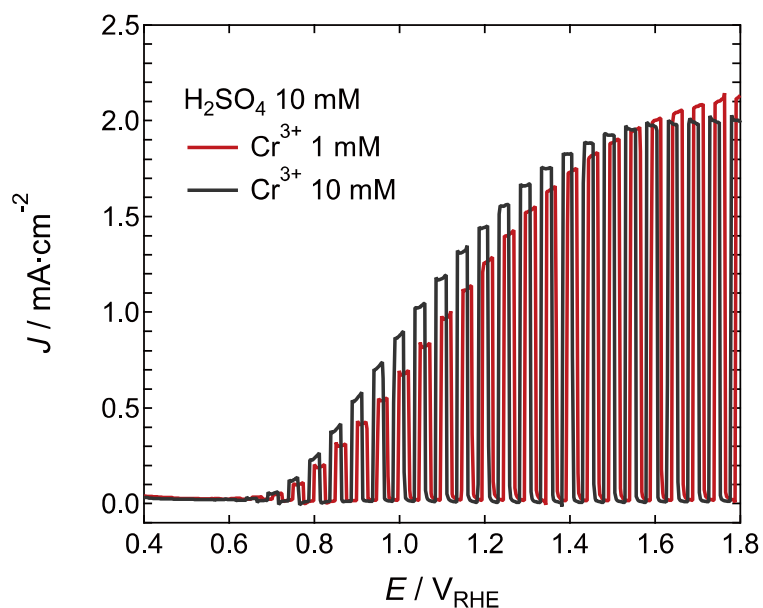


Fig. S8: J - V curves under chopped simulated sunlight at 1 Sun in 1 and 10 mM Cr³⁺ and 10 mM H₂SO₄ electrolytes from the backside of the WO₃ photoanode.

ABPE for the Cr⁶⁺ production

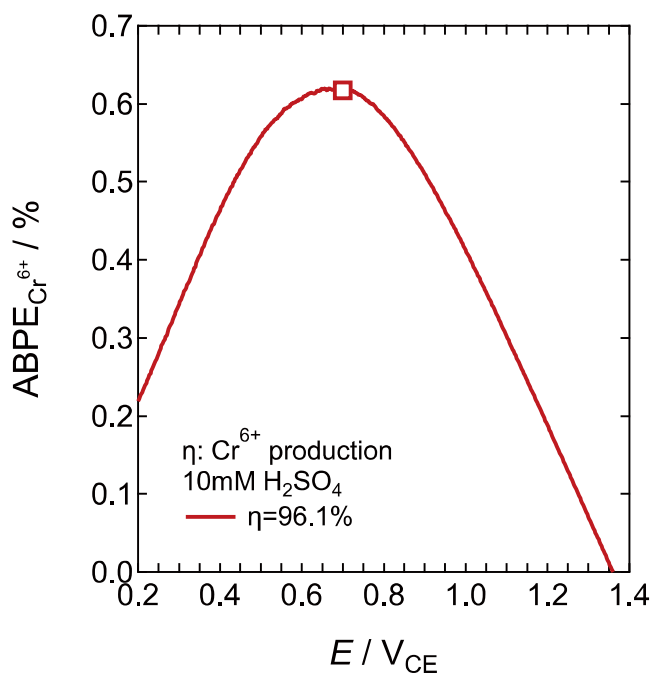


Fig. S9: ABPE_{Cr⁶⁺} calculated for the evolution of Cr⁶⁺ in 10 mM Cr³⁺ and 10 mM H₂SO₄ electrolyte under the simulated solar light illumination. The solid line was calculated curve by using the faradaic efficiency (96.1%) evaluated at 0.7 V_{CE}. The open square represents the calculated by observed value at 0.7 V_{CE}.

Stability of the stored Cr³⁺ solution

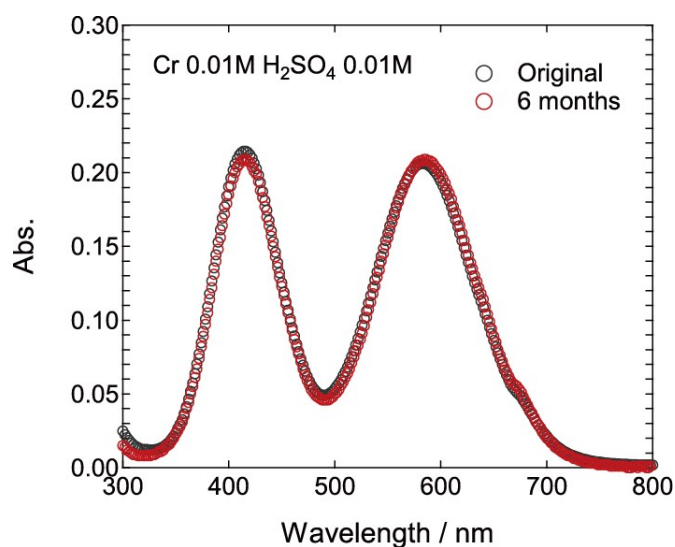


Fig. S10: The storage time dependence of absorption spectra of the 10 mM Cr³⁺ and 10 mM H₂SO₄ solution. The aqueous sulfuric acid Cr³⁺ solutions can be stably stored for long period.

Chromic acid oxidation experiments: Evaluation of concentrations for *p*-benzendiol and *p*-benzoquinone

The production of *p*-benzoquinone from *p*-benzendiol using the photoelectrochemically obtained Cr⁶⁺ ions was evaluated by colorimetry by using the UV-VIS spectroscopy. The absorption spectra of reference solutions for the *p*-benzoquinone and *p*-benzendiol in the aqueous sulfuric acid were measured. In addition to these reference spectra, the absorption spectra for Cr³⁺ and Cr⁶⁺ in the aqueous sulfuric acid (Fig. S5) were also used for the analysis. The reference spectra were deconvoluted, and those spectral shapes were expressed as $f_D(\lambda)$ for the *p*-benzendiol and $f_Q(\lambda)$ for the *p*-benzoquinone. For the concentration analysis of the *p*-benzoquinone and *p*-benzendiol in the test solutions, the absorption spectra were fitted by following equation:

$$f(\lambda) = c_D f_D(\lambda) + c_Q f_Q(\lambda) + (c_{III} - c_{VI}) f_{III}(\lambda) + c_{VI} f_{VI}(\lambda)$$

where the c_D and c_Q represent the concentrations of *p*-benzendiol and *p*-benzoquinone. Figure S10c shows one example of fitted test solution (after 0.2 mM *p*-benzendiol was added to 298.5 μ M Cr⁶⁺ contained Cr³⁺/H₂SO₄ solution) by using this equation. The spectral curve was fitted very well and the c_D and c_Q were evaluated with satisfactory accuracy.

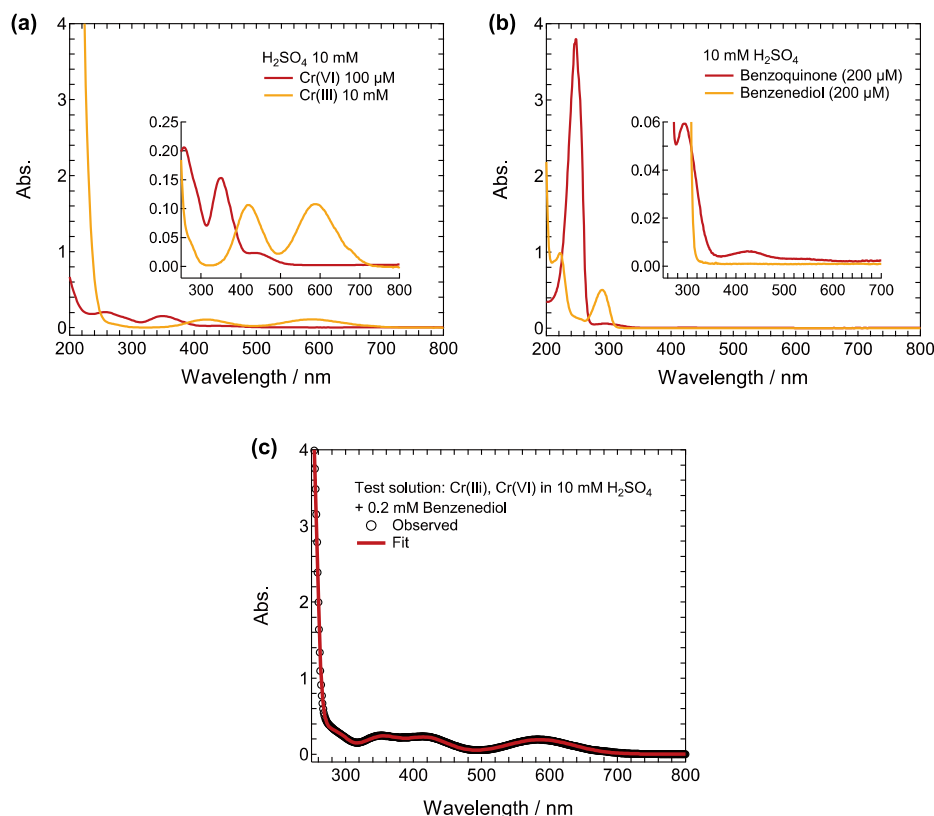
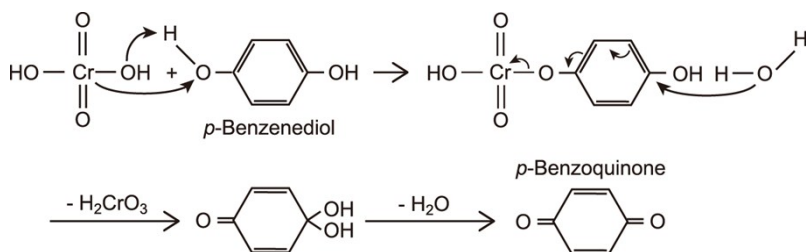


Fig. S11: The absorption spectra for (a) Cr³⁺ and Cr⁶⁺ contained aqueous sulfuric acid solutions and (b) *p*-benzoquinone and *p*-benzenediol contained aqueous sulfuric acid solutions. (c) The fitted spectral curve of test solution after the chromic acid oxidation reaction.

Reaction process of *p*-benzoquinone from *p*-benzenediol by Cr(VI) ions

Two hydroxyl groups in the *p*-benzenediol are attacked from the Cr(VI) acid ions as follows:



Through the oxidation process of hydroxyl groups by the Cr(VI) ions, the Cr(IV) ions (H₂CrO₃) are intermediately produced. The oxidation of alcohol by the Cr(IV) could additionally proceed via several processes as reported in ref. 3.

References

- Chromium Statistics and Information, U.S. Geological Survey, <https://minerals.usgs.gov/minerals/pubs/commodity/chromium/>
- Risk Assessment of Chemical Substances, Ministry of Environment, Government of Japan, <http://www.env.go.jp/chemi/report/h24-01/index.html> (in Japanese)
- M. Rahman and J. Roček, *J. Am. Chem. Soc.*, 1971, **93**, 5455.